

ChemSusChem

Supporting Information

Monomers from CO₂: Superbases as Catalysts for Formate-to-Oxalate Coupling

Eric Schuler,* Pavel A. Ermolich, N. Raveendran Shiju, and Gert-Jan M. Gruter*© 2021 The Authors. ChemSusChem published by Wiley-VCH GmbH. This is an open access article under the terms of the Creative Commons Attribution Non-Commercial NoDerivs License, which permits use and distribution in any medium, provided the original work is properly cited, the use is non-commercial and no modifications or adaptations are made.

Table of Contents

Section 1: Experimental details	Page 3
Section 2: Details on mechanistic investigations	Page 6
Section 3: Details on reaction kinetics	Page 7
Section 4: References	Page 9

SUPPORTING INFORMATION

Section 1: Experimental details**Reagents**

All chemicals (Potassium formate, Sodium formate, Potassium oxalate, Sodium formate, Potassium hydride, Sodium hydride, Lithium hydride, Sodium amide, Potassium hydroxide, Sodium borohydride) were obtained from commercial suppliers (Sigma-Aldrich®), dried and stored in a dry environment. Otherwise, the chemicals were not further processed.

Sample preparation

Potassium and sodium formate were dried overnight in a vacuum oven at 110 °C and transferred to the glove box. Hydride catalysts were transferred to the glove box directly and washed with dry hexane if needed to remove the protective wax film and subsequently dried under vacuum. Reaction mixtures for catalyst screening were prepared in batches of different weight percent ratios of catalyst to formate. For each batch, 3-5 g of dry potassium or sodium formate or potassium oxalate were crushed in a ceramic mortar until a fine powder was obtained. After 5 minutes of mixing the batch was transferred to a glass vial with a plastic septum cap. Different weight percent of catalyst (0.01, 0.5, 1, 2.5, 5, 10, 25 wt.%) were weighed and mixed with the formate. Standard batch size was 5 g to reduce weighing error. For each reaction, 290-310 mg of the mixture was used. The exact mass was measured and used to calculate theoretical yields of produced gases and solids. The samples for oxalate decomposition were prepared following the same procedure.

Kinetic measurements

The kinetics of the reactions were studied by time-resolved volumetric measurements of the produced gas during reaction. This was performed with a self-build digital kinetic evaluation device called 'Bubble-Counter' and was first described in 2019.^[1] This device was invented by Thierry Slot (HIMS, UvA) and is capable of measuring gas production over time (so-called "bubble counting") and heating of the sample using an internal PID loop. Each gas bubble is recorded as a string of values. The gases are subsequently qualitatively analyzed using MS or GC. The string includes the time when the bubble was counted, its bubble size and the corresponding temperature value of a thermocouple. The thermocouple can be placed on the heating element or inside the reactor. This way the reaction can be studied in a broad temperature range with high time resolution.

For all experiments, 7 mL glass vials were used as reactors in a ring-shaped heating element connected to the PID controller in the "Bubble-Counter" device.

Non-isothermal measurements

For non-isothermal measurements, the reaction vial was ramped to a setpoint temperature with either 0.2 °C min⁻¹, 2 °C min⁻¹ or 5 °C min⁻¹ heating rates. For reactions at lower temperatures with NaH, KH, LiH, and NaNH₂ the reaction vessel was heated from room temperature to 210 °C with the same ramping rate. For higher temperature reactions using KOH or NaBH₄ as catalyst reaction was ramped from room temperatures to 420 °C. After holding the sample for 20 min at the reached temperature, the reactor was taken out and cooled to the room temperature. The remaining catalyst was then quenched with 1 mL of distilled water.

Isothermal experiments

For isothermal experiments, the heating element was preheated to the desired reaction temperature. Each reactor was inserted in the heating element and taken out with 15-60 s intervals between the samples. After the reaction, samples were immediately quenched in the ice bath, weighed inside the glove box and quenched with 1 mL of distilled water.

Oxalate decomposition

For the decomposition reaction of oxalate, the reaction mixture was heated to 450 °C with a heating rate of 5 °C min⁻¹.

Reaction order:

To estimate the reaction, order the formulas beneath were used. The reaction order is defined as a dependence of the rate of a chemical reaction on the concentrations of the reactants.^[2]

For formate coupling this can be written as:

SUPPORTING INFORMATION

$$\text{rate} = k * [\text{Formate}]^n \quad (\text{Eq. S1})$$

Where k and n are the reaction rate constant and reaction order with respect to the formate concentration. To experimentally determine the reaction, order the following formulae can be implemented:

$$(\text{observed}) \text{ rate} = k * [\text{reactant}]^n \quad (\text{Eq. S2})$$

Taking the natural log of both sides of the equation (Eq. S2) gives:

$$\ln(\text{rate}) = \ln(k * [\text{reactant}]^n) \quad (\text{Eq. S3})$$

After rearrangement:

$$\ln(\text{rate}) = \ln(k) + n * \ln([\text{reactant}]) \quad (\text{Eq. S4})$$

Now if one plots $\ln(\text{rate})$ vs. $\ln([\text{reactant}])$, using (Eq. S4), the resulted graph should look like a linear function. The slope of the graph accounts for the reaction order. From the intercept one can derive a rate constant of the reaction k .^[3]

Activation energy

To determine the activation energy one can use the linear logarithmic form of the Arrhenius equation:

$$\ln(k) = \ln(A) - \frac{E_a}{R} \times \frac{1}{T} \quad (\text{Eq. S5})$$

It uses the dependency of a logarithm of reaction constant k on the reciprocal temperature. Plotting the $\ln k$ against $1/T$ produces a straight line. The slope represents the activation energy, whilst the intercept leads to the pre-exponential factor A . This pre-exponential factor is often referred to as “frequency” factor A and indicates the rate at which molecular collisions occur.^[2]

Raman:

We used a Tornado Hyperflux Pro Raman spectrometer equipped with an Axiom RFP 400 probe and a laser with a 785 nm wavelength. A hole on the bottom of the heating element was used to access the reactor from the bottom during the reaction. A time resolution of 900 ms was realized. During the reaction, also the volume and composition of the gases were analyzed online. We used this system to follow the reaction and further confirm the reaction progression by an additional mean.

Characterization

Products were characterized using different absorbance bands of oxalate, formate, and carbonate in FTIR spectroscopy. To ensure high-quality results, random samples were double-checked with liquid chromatography and ion chromatography. The produced gases were determined by mass spectrometry and gas chromatography. ¹H NMR and ¹³C NMR spectroscopy were implemented to confirm molecular structures and presence of intermediates. Isotope labeling, combined with mass spectrometry was used to identify possible carbonite intermediate. Raman spectroscopy was used to identify possible reaction mechanism and follow the reaction time-resolved spectroscopically.

Liquid cell infrared

We used a SmartSeal liquid cell from PIKE technologies with CaF₂ windows and cavity thickness of 0.025 mm. The spectra were recorded with a Varian 660-IR spectrometer.

The cell was flushed with nitrogen gas for 5 - 10 min before measurement. After scanning the background of the cell, the water sample was scanned as a reference. Each sample was scanned thrice in the 400 – 4000 cm⁻¹ range to ensure the reproducibility. After each measurement, the cell was flushed with deionized water to remove traces of the previous sample out. The sample volume for the IR measurement was around 0.5 mL.

The resulted spectra were analyzed with a self-developed deconvolution program. A set of selected spectra was examined in the 1250 – 1400 cm⁻¹ wavenumber range and fitted with simulated spectrum. In figure S1 an example is presented. The simulation was based on a Limited-memory BFGS algorithm.^[4,5]

SUPPORTING INFORMATION

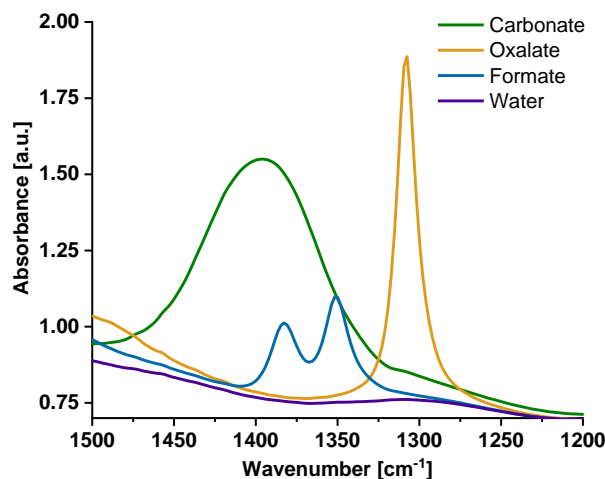


FIGURE S1 IR spectra of the main components of the reaction. All three mixture components have different absorbance bands. This allows to use Beer-Lambert law to deconvolute the mixture spectra after the reaction.

Above mentioned results were then recalculated using the following formulae to obtain the exact concentration of the species present after the reaction:

$$\text{mol of product in original sample} = \text{concentration product (M)} \times \text{dilution coefficient} \quad (\text{Eq. S6})$$

$$\text{Conversion} = \frac{\text{mol used formate} - \text{mol unreacted formate}}{\text{mol used formate}} \quad (\text{Eq. S7})$$

$$\text{Selectivity oxalate} = \frac{\text{mol oxalate} \times 2}{\text{mol used formate} - \text{mol unreacted formate}} \quad (\text{Eq. S8})$$

$$\text{Selectivity carbonate} = \frac{\text{mol carbonate}}{\text{mol used formate} - \text{mol unreacted formate}} \quad (\text{Eq. S9})$$

$$\text{Selectivity other} = 1 - (\text{Selectivity oxalate} + \text{Selectivity carbonate}) \quad (\text{Eq. S10})$$

Liquid chromatography

For product analysis with liquid chromatography the dissolved samples were diluted with purified water to a maximum salt concentration of 1 mg/ml. We use an internal standard and a Agilent 1200 series HPLC with a diode array detector.

Mass spectrometry

To study the gas species evolving from the formate coupling reactor online we used a Pfeiffer Vacuum Omnistar GSD 330 01 to analyze the off-gases of the reactor.

Mass spectra for the mechanistic studies were collected on an AccuTOF LC, JMS-T100LP Mass spectrometer (JEOL, Japan). For these measurements, reaction products were quenched with deuterium oxide (D_2O) instead of deionized water. It was expected that formed carbonite ions – if any – after quenching with D_2O will transform into deuterated formate. Deuterated formate could be observed at different mass to charge ratio in the MS spectrum. The measurement conditions in the mass spectrometer for Positive and Negative-ion mode were: Needle voltage 2500 V, Orifice 1 voltage 120 V, Orifice 2 voltage 9 V, Ring Lens voltage 22 V. Orifice 1 80 °C, Desolvating Chamber 250 °C. Flow injection with a flow rate of 0.01 mL/min. All mass spectra were recorded with an average duration of 0.5 min.

SUPPORTING INFORMATION

Gas chromatography

We use an Agilent 7820A GC system equipped with Hayesep Q and a Molecular sieve 5A column to analyse the gases originating from the formate coupling reactions. Both online measurements and cumulative measurements with a mix of all produced gases were performed.

Nuclear magnetic resonance

NMR spectra were recorded on a Bruker AMX 300 (300.1 MHz and 75.5 MHz for ^1H and ^{13}C respectively) and Bruker AMX 400 (400.1 MHz and 100.6 MHz for ^1H and ^{13}C respectively).

Differential scanning calorimetry

Differential scanning calorimetry (DSC) measurements were used to determine the melting points of the reaction mixtures. A Mettler Toledo DSC 3+ was used with aluminum crucibles. The samples were prepared in the glove box to prevent contact with moisture. Samples were tested for melting point in a range from 25 to 300 °C at a heating rate of 1 °C/min.

Turnover frequency

To determine the turnover frequency at a specific reaction temperature, the intrinsic molar reaction rate is corrected by amount of catalyst present during the reaction. The amount of catalyst present is expressed in molar loading :

$$\text{TOF} = (\text{Intrinsic rate (mol/s)}) / (\text{catalyst loading (mol)}) \quad (\text{Eq. S11})$$

Section 2: Details on mechanistic investigations

Isotopic labeling experiments

For the isotope labeling experiments we performed a potassium formate coupling reaction with hydrides in excess (e.g. 10 wt.% NaH). After completion of the reaction, the solid mixture was quenched with D_2O . The remaining carbonite in the solid then reacts with the D_2O to form deuterated formate. As standards we also added D_2O to dry potassium formate and the potassium formate / hydride mixture without performing the reaction. The liquid samples were analyzed using AccuTOF LC, JMS-T100LP Mass spectrometer with electrospray ionization as described above. For deuterated formate ions we expect a m/z value of 46. For conventional formate we expect a m/z value of 45. Oxalate, which is present in the sample after reaction, is expected to be instable with ESI due to the close proximity of the charges in the molecule.

The major Peak in the mass spectrum for the quenched formate coupling reaction was 46 m/z , indicating the sole presence of deuterated formate as shown in figure S2. None of the control experiments showed the presence of a 46 m/z signal, but a signal at 45 m/z .

SUPPORTING INFORMATION

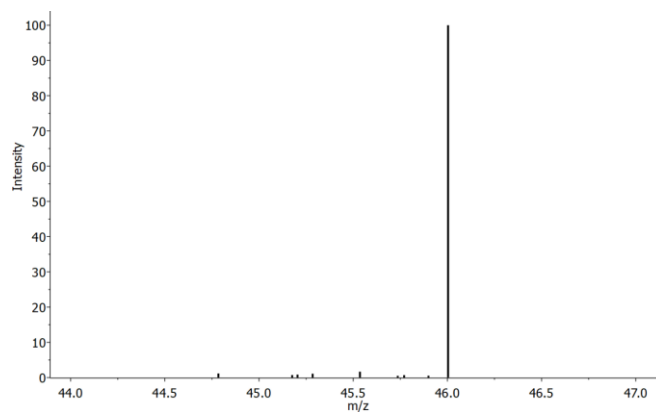


Figure S2 Mass spectrum of deuterium labelled formate after reaction. Peak at 46 m/z is indicative for deuterated formate (DCOO^-). No non-labelled formate (HCOO^-) with 45 m/z was observed in the sample.

SUPPORTING INFORMATION

Section 3: Details on reaction kinetics

Operando Raman experiments

We follow the reaction by time-resolved Raman over the full reaction time. The conversion of formate to oxalate can be observed. The Carbonite signal which was seen by Lakkaraju *et al.* could not be observed in any of our many attempts.^[6] The figure below shows the set-up:

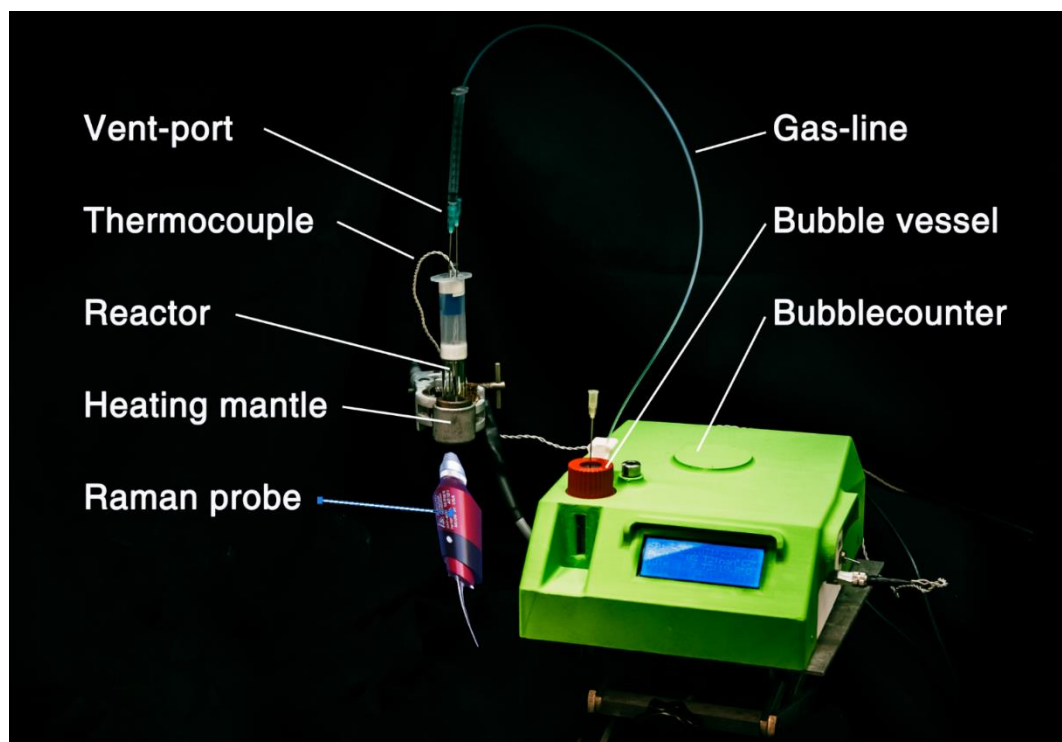


Figure S3 The bubble counter coupled with operando raman set-up for mechanistic and kinetic experiments. The bubblecounter both counts produced gas bubbles and controls the heating mantle. Reactor and bubble vessel are connected via a gas line; inert conditions are kept as the bubble vessel functions as an airlock.

Foaming during formate coupling reaction

The physical structure of the reaction product depends on the heating rate of the reaction. We tested different heating rates and in figure S3 below the compact solid, achieved with slow heating rates, and puffed up structure, resulting from fast heating rates. Are shown.



Figure S4 With slow heating at 0.5 °C/min the product forms a compact solid (left). With fast heating in a pre-heated reactor at 200 °C, a puffed-up foam was obtained (right).

Activation energies obtained from kinetic experiments

The activation energies were calculated for various potential reaction orders and different catalyst loadings. The full list of calculated activation energies, errors and pre-exponential factors are presented below.

SUPPORTING INFORMATION

Table S1 Activation energy and pre-exponential factors for formate coupling using different catalysts.

Catalyst	Catalyst Loading (wt. %)	Activation energy (kJ mol ⁻¹)				Temperature range (onset Temp) (°C)	Pre-exponential factor A (s ⁻¹)	Error (± kJ mol ⁻¹)
		Observed rate	Intrinsic rate (<i>k</i>)					
			0 order	1 order	2 order			
NaH	0.5	535	535	576	609	157 – 162	5.62 × 10 ⁶⁷	5.68
	1.0	516	516	559	603	157 – 162	1.39 × 10 ⁶⁵	
	2.5	530	530	587	643	157 – 162	2.06 × 10 ⁶⁷	
KH	2.5	546	546	558	576	152 – 155	4.15 × 10 ⁶⁸	5.54
	1.0	527	527	536	544	155 – 160	2.79 × 10 ⁶⁶	
	5.0	534	534	577	619	157 – 162	5.62 × 10 ⁶⁷	
LiH	1.0	831	831	921	1011	161 – 163	7.22 × 10 ⁸⁶	11.1
	5.0	793	793	801	810	152 – 154	9.77 × 10 ⁸⁵	
	10.0	818	818	841	856	153 – 158	2.65 × 10 ⁸⁶	
NaNH ₂	2.5	330	330	341	355	157 – 162	2.87 × 10 ⁵⁶	25.5
	1	279	279	294	305	155 – 162	4.92 × 10 ⁴¹	
KOH	5	125	125	129	133	318 – 348	1.06 × 10 ¹³	-
HCOOK	0	196	196	202	208	363 – 409	1.28 × 10 ¹⁹	-

Below you find examples for Arrhenius plots to calculate the activation energies of different formate coupling reactions.

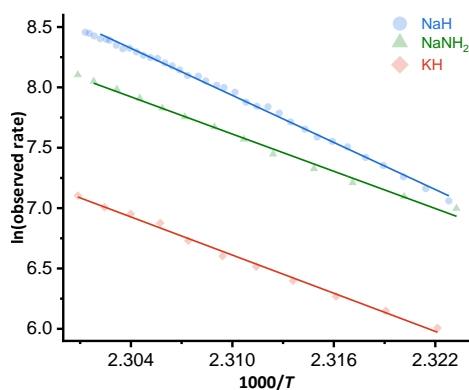


Figure S5 Arrhenius plots for the hydride and amide catalysed reactions. More gas was produced with NaH, indicating that NaH is more active in the formate coupling. NaNH₂ showed similar behaviour with lower activation energies.

SUPPORTING INFORMATION

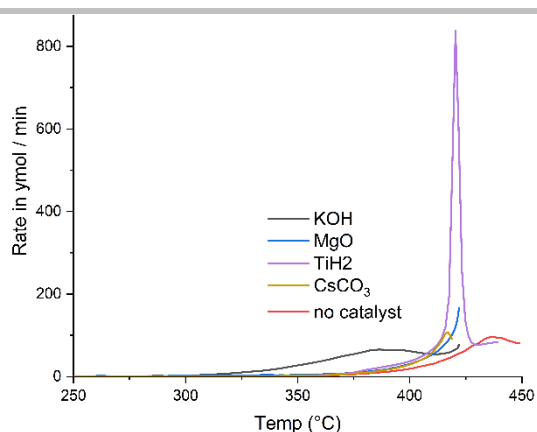


Figure S6 Rate of Hydrogen evolution during FCR with potassium formate observed with catalysts that showed no catalytic activity. KOH was added as a comparison.

Section 4: References

- [1] T. K. Slot, N. R. Shiju, G. Rothenberg, *Angew. Chemie - Int. Ed.* **2019**, *58*, 17273–17276.
- [2] P. Atkins, J. de Paula, *Physical Chemistry*, **2006**.
- [3] I. Chorkendorff, J. W. Niemantsverdriet, in *Concepts Mod. Catal. Kinet.*, **2007**, pp. 23–78.
- [4] R. Malouf, in *Proc. 6th Conf. Nat. Lang. Learn. - Vol. 20*, Association For Computational Linguistics, Stroudsburg, PA, USA, **2002**, pp. 1–7.
- [5] G. Andrew, J. Gao, in *Proc. 24th Int. Conf. Mach. Learn.*, ACM, New York, NY, USA, **2007**, pp. 33–40.
- [6] P. S. Lakkaraju, M. Askerka, H. Beyer, C. T. Ryan, T. Dobbins, C. Bennett, J. J. Kaczur, V. S. Batista, *ChemCatChem* **2016**, *8*, 3453–3457.